

## EFFECT OF Ce DOPING ON THE CHARACTERISTIC PROPERTIES OF CdS NANOPARTICLES

A. EKINCI<sup>a</sup>, S. HOROZ<sup>b,\*</sup>, Ö. ŞAHİN<sup>c</sup>

<sup>a</sup>*Department of Occupational Health and Safety, Siirt School of Health, Siirt University, 56100 Siirt, Turkey*

<sup>b</sup>*Department of Electrical and Electronics Engineering, Faculty of Engineering, Siirt University, 56100 Siirt, Turkey*

<sup>c</sup>*Department of Chemical Engineering, Faculty of Engineering, Siirt University, 56100 Siirt, Turkey*

In our present study, Ce doped CdS nanoparticles were synthesized in room temperature environment by using chemical co-precipitation technique which is cheap in cost. Ce doped CdS nanoparticles ( average particle size: 3.7 nm) were found to have cubic structure as a result of XRD measurements. It has also been clearly observed that Ce dopant ions do not alter the structure of the host semiconductor CdS. Using the spectrum obtained as a result of UV-Vis measurement, the energy band gap of Ce doped CdS nanoparticles was determined as 2.73 eV. This value was observed to be higher than the energy band gap of bulk CdS (2.42 eV). Thus, it can be said that this change in the energy band gap is due to the quantum confinement effect. The maximum IPCE value was 27% for Ce doped CdS nanoparticles while the IPCE values was 4% for pure CdS nanoparticles, respectively. The IPCE of the solar cells improves with the Ce dopant ion. Moreover, the spectral response range of Ce doped CdS nanoparticles widens with the Ce dopant ion. This is attributed to the long lifetimes of the Ce<sup>3+</sup> excited states that facilities the transfer of the charge carries to the photoelectrode.

(Received January 30, 2020; Accepted June 2, 2020)

**Keywords:** Application, Characterization, Doping, Rare-earth element, Synthesis

### 1. Introduction

Rare earth doped semiconductors, known as phosphorus materials, are of great importance in the use of optical display devices. It is possible to obtain the blue, green and red colors that exist in full color devices with rare earth ions (1-4). Therefore, various studies have been carried out on the investigation of properties of different rare earth element doped II-VI semiconductor materials (5-8). The characteristics of dopant mainly affect the luminescence properties of rare earth element doped II-VI semiconductors (9, 10). The electronic structure of rare earth ions with uncharged 4f<sup>n</sup> shells differs from other elements. The 4s<sup>2</sup> and 4p<sup>6</sup> orbitals protect the 4f<sup>n</sup> electrons (11, 12). Excitation of materials doped with rare earth ions leads to sharp line emission. This emission can be seen in the UV, Vis and IR regions of the spectrum (13).

The reason why the rare earth ions have not been successfully incorporated into the CdS is due to the large radius and charge mismatch between the rare earth ions and the Cd<sup>2+</sup> ions. This leads to inefficient energy transfer (14-16). Many lanthanum doped materials were prepared in nanoscale and their properties were investigated (17-19). The weakness of these studies is the synthesis of these nanoparticles by subjecting them to high temperature processes. However, contrary to these studies, it is emphasized that cerium ions doped semiconductor materials have lower particle size and higher surface area (20). Ce doped CaS (21, 22) and Ce doped SrS (23, 24) nanoparticles were synthesized using different synthetic techniques such as solid state diffusion and chemical co-precipitation, and data on their characteristic properties (structural, morphological and optical) were reported. To date, no experimental studies have been conducted on the investigation of the photovoltaic properties of Ce doped CdS nanoparticles.

\* Corresponding author: sabithoroz@siirt.edu.tr

In our present study, Ce doped CdS nanoparticles were synthesized in room temperature environment by using chemical co-precipitation technique which is cheap in cost. The nanoparticles obtained as a result of the experimental study were characterized by x-ray diffraction (XRD) (for structural properties), photoluminescence (PL) (for optical properties), UV-Vis (for optical properties), the incident photon to current conversion efficiency (IPCE) and current density- voltage (J-V) (for photovoltaic properties), respectively.

## 2. Synthesis process

Cerium nitrate, cadmium acetate and sodium sulfide are commercial solid chemicals used in the synthesis of Ce doped CdS nanoparticles. In the synthesis process, de- ionized water and ethylene diamine were used as solvents. 2.66 g of cadmium acetate salt was dissolved in the solvent containing ethylene diamine and de- ionized water. Stirring was continued at room temperature until the salt used as the cadmium source was completely dissolved. 0.78 g of sodium sulfide salt was added to a 100 mL beaker containing cadmium aqueous solution. The color of the solution was observed to be orange after the addition. The stirring was stopped until a homogeneous mixture was obtained, allowing solid CdS to precipitate. The wet CdS precipitate was removed from the solvent with the aid of filter paper. The CdS precipitate on the filter paper was washed several times with purified water and ethanol, respectively. After washing, the wet CdS precipitation was dried in the oven. To synthesize Ce doped CdS nanoparticles using chemical precipitation technique; 0.13 cerium nitrate salt was added to the solution containing 2.66 g of cadmium acetate and all the above steps were followed.

Ce doped CdS nanoparticles synthesized using chemical co-precipitation technique which is an inexpensive and simple method were characterized by x-ray diffraction (XRD) (for structural properties), photoluminescence (PL) (for optical properties), UV-Vis (for optical properties), the incident photon to current conversion efficiency (IPCE) and current density- voltage (J-V) (for photovoltaic properties), respectively.

## 3. Results and discussion

The x-ray diffraction patterns of undoped and Ce doped CdS nanoparticles are shown in Fig. 1. The diffraction peaks are significantly broadened due to very small size of the nanoparticles. Fig. 1 indicates three diffraction peaks at  $2\theta$  values;  $26.5^\circ$ ,  $42.9^\circ$  and  $50.4^\circ$  corresponding to reflections from (111), (220) and (311) crystal planes of the cubic zinc blend phase and are well matched with the standard cubic CdS (JCPDS card No. 10-454). No characteristics peaks corresponding to impurity phases were detected. Using the Debye-Scherer formula (25) average particle size of nanoparticles was calculated to be about  $3.7 \pm 0.5$  nm.

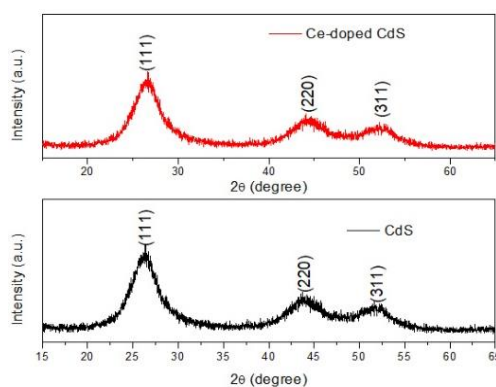
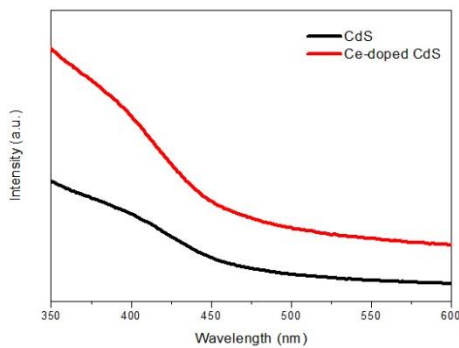


Fig. 1. XRD spectra of nanoparticles.

The UV-Vis absorption spectra of Ce doped CdS nanoparticles synthesized by chemical co-precipitation at room temperature are shown in Fig. 2. The absorption edge of the Ce doped CdS nanoparticles was determined using the optical spectra obtained. Extrapolating the linear region of the spectra was used to determine the energy band gap value of Ce doped CdS nanoparticles. Broad and less symmetric absorption peaks of pure CdS and Ce doped CdS nanoparticles were observed at about 449 nm and 453 nm, respectively, that is effectively blue shifted compared to the bulk band gap wavelength at 515 nm. Blue shifting absorption peak is attributed to the quantum size effect (15), whereas the broadening and asymmetry are due to the wide size distribution of synthesized particles. Different size of particles give number of excitonic peaks that appear at different energies and overlapping of these peaks produces a broadening in absorption spectra.



*Fig. 2. UV-Vis absorption spectra of nanoparticles.*

As shown in Fig. 3, when excitation wavelength is used as 320 nm, it was observed that both pure CdS and Ce doped CdS nanoparticles have an emission band around 350-450 nm. No emission peaks of defects were found in both samples. An important observation should be noted that the emission band of Ce doped CdS nanoparticles shifts to longer wavelengths than that of pure CdS (from 360 nm to 374 nm). With this result, it can be said that the Ce doped metal has a positive effect on the luminescence property of CdS. It is possible to see similar observations in different studies carried out on the optical properties of CdS nanoparticles (26-28).

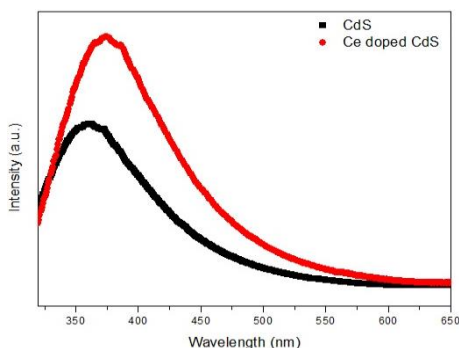


*Fig. 3. Emission spectra of nanoaparticles.*

J-V curves of pure CdS and Ce doped CdS nanoparticles are indicated in Fig. 4. As shown in Fig. 4, it can be said that owing to Ce dopant metal, the short circuit current density and the conversion efficiency of Ce doped CdS nanoparticles is better than the pure sample. The calculated photoelectric conversion efficiency (%) and short circuit current density for pure CdS and Ce doped CdS nanoparticles are  $3.71 \text{ mA/cm}^2$ ,  $6.43 \text{ mA/cm}^2$ , 0.71% and 1.11%, respectively. The reasons for the increase of the conversion efficiency of the solar cell can be comprehended from one aspect. (1) Compared with pure CdS and Ce doped-CdS nanoparticles, cosensitization of

double doped CdS nanoparticles can better increase the range and intensity of the absorption spectrum of the solar cell, improve the utilization rate of the incident light, improve the rate of capture of the photons, and increase the photocurrent density and the open circuit voltage, and double doped CdS electrode had lower dark current which was benefited for delivery of the electrons, inhibited for recombination of the electrons, thus ultimately improving photoelectric conversion efficiency of the solar cell.

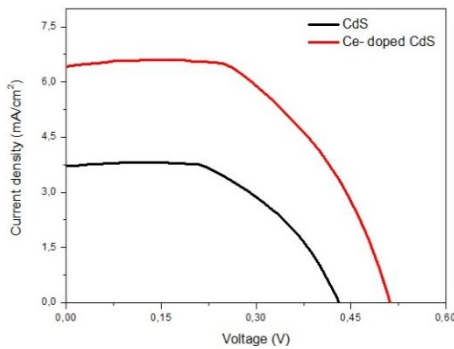


Fig. 4. J-V curves of nanoparticles.

At least, the IPCE curves of pure CdS and Ce doped CdS nanoparticles shown in Fig. 5 were discussed. At the wavelength of 400 nm, the maximum IPCE value was 27% for Ce doped CdS nanoparticles while the IPCE values was 4% for un-doped CdS nanoparitcles, respectively. The IPCE of the solar cells clearly improves with the Ce dopant ion. Moreover, the spectral response range of Ce doped CdS nanoparticles widens with the Ce dopant ion. This is attributed to the long lifetimes of the  $\text{Ce}^{3+}$  excited states that facilities the transfer of the charge carries to the photoelectrode.

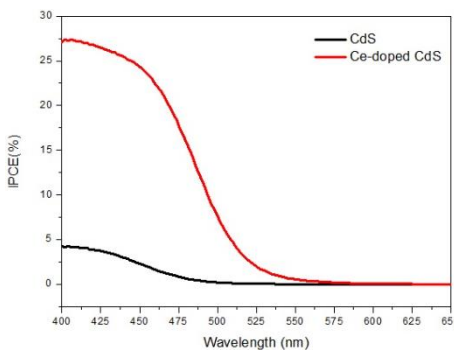


Fig. 5. IPCE curves of nanoparticles.

#### 4. Conclusions

In our present study, Ce doped CdS nanoparticles were synthesized in room temperature environment by using chemical co-precipitation technique which is cheap in cost. The average particle size of Ce doped CdS nanoparticles, which were found to have a cubic structure, was calculated as 3.7 nm. The absorption peaks of pure CdS and Ce doped CdS nanoparitcles were observed at about 449 nm and 453 nm, respectively , that is effectively blue shifted compared to the bulk band gap wavelength at 515 nm. Blue shifting absorption peak is attributed to the quantum size effect. it was observed that both pure CdS and Ce doped CdS nanoparticles have an emission band around 350-450 nm.

An important observation should be noted that the emission band of Ce doped CdS nanoparticles shifts to longer wavelengths than that of pure CdS ( from 360 nm to 374 nm). In

terms of application, the power conversion efficiency (%) and IPCE (%) values of Ce doped CdS nanoparticles-based solar cell devices were calculated as 1.11 and 27, respectively, while those values for pure CdS were 0.71 and 4, respectively. Clearly, the Ce dopant element plays an active role in improving the efficiency of Ce doped CdS-based solar cell devices.

## References

- [1] S. Horoz, B. Yakami, U. Poudyal, J. M. Pikal, W. Wang and J. Tang, AIP Advances **6** (4), 045119 (2016).
- [2] S. Khajuria, S. Sanotra, J. Ladol and H. N. Sheikh, Journal of Materials Science: Materials in Electronics **26** (9), 7073-7080 (2015).
- [3] Y. Wang, G. Zhu, S. Xin, Q. Wang, Y. Li, W. Quansheng, C. Wang, X. C. W, X. Ding and W. Geng, Journal of Rare Earths **33** (2015).
- [4] S. Horoz, Superlattices and microstructures **111**, 1043-1049 (2017).
- [5] N. Jeevanantham and O. N. Balasundaram, Journal of Materials Science: Materials in Electronics **29** (16), 14073-14083 (2018).
- [6] C. A. Ortiz, A. L. Giraldo-Betancur, M. A. Hernández-Landaverde, M. Ramírez-Cardona, A. Mendoza-Galván and S. Jiménez-Sandoval, Journal of Vacuum Science & Technology A **35** (3), 031505 (2017).
- [7] J. Y. Park, D.-W. Jeong, K.-M. Lim, Y.-H. Choa, W.-B. Kim and B. S. Kim, Applied Surface Science **415**, 8-13 (2017).
- [8] B. Poornaprakash, U. Chalapathi, M. Reddeppa and S.-H. Park, Superlattices and Microstructures **97**, 104-109 (2016).
- [9] R. Röder, S. Geburt, M. Zapf, D. Franke, M. Lorke, T. Frauenheim, A. L. da Rosa and C. Ronning, physica status solidi (b) **256** (4), 1800604 (2019).
- [10] S. Horoz, Journal of Materials Science: Materials in Electronics **29** (9), 7519-7525 (2018).
- [11] H. J. Lozykowski, W. M. Jadwisienczak and I. Brown, Journal of Applied Physics **88** (1), 210-222 (2000).
- [12] S. G. Semenov, M. E. Bedrina, A. E. Buzin and A. V. Titov, Russian Journal of General Chemistry **89** (7), 1424-1432 (2019).
- [13] M. Ayvacıklı, A. Ege, S. Yerci and N. Can, Journal of Luminescence **131**, 2432–2439 (2011).
- [14] F. Ben Slimen, Z. Zaaboub, M. Haouari, N. Mohamed, H. Ben Ouada, S. Chaussédent and N. Balu-Gaumer, RSC Adv. **7**, 14552-14561 (2017).
- [15] S. L, J. R, P. A, L. Jih-Hsin and M. Hsin-Yuan, Powder Technology **266**, 407-411 (2014).
- [16] S. S. Talwatkar, A. L. Sunatkari, Y. S. Tamgadge, V. G. Pahurkar and G. G. Muley, Journal of Nanostructure in Chemistry **5** (2), 205-212 (2015).
- [17] A. Manikandan, E. Manikandan, B. Meenatchi, S. Vadivel, S. K. Jaganathan, R. Ladchumananandasivam, M. Henini, M. Maaza and J. S. Aanand, Journal of Alloys and Compounds **723**, 1155-1161 (2017).
- [18] G. Murtaza, S. M. A. Osama, M. Saleem, M. Hassan and N. R. K. Watoo, Applied Physics A **124** (11), 778 (2018).
- [19] A. Ekinci, O. Sahin and S. Horoz, Journal of Materials Science: Materials in Electronics **29** (6), 5233-5238 (2018).
- [20] G. Guo, D. Li, Z. Wang and H. Guo, Journal of Rare Earths **23**, 362-366 (2005).
- [21] P. I. Paulose, J. Joseph, M. K. Rudra Warrier, G. Jose and N. V. Unnikrishnan, Journal of Luminescence **127** (2), 583-588 (2007).
- [22] Z. Qiu, H. Lian, T. Luo, J. Fan, X. Cai, Z. Cheng, M. Shang, S. Lian and J. Lin, CrystEngComm **17** (45), 8676-8682 (2015).
- [23] S. Rekha and E. I. Anila, Journal of Fluorescence **28** (5), 1029-1036 (2018).
- [24] A. Vij, S. P. Lochab, S. Singh, R. kumar and N. Singh, Journal of Alloys and Compounds **486** (1), 554-558 (2009).
- [25] H. P. Klug and L. E. Alexander, X-Ray Diffraction Procedures: For Polycrystalline and Amorphous Materials, 2nd Edition, by Harold P. Klug, Leroy E. Alexander, pp. 992. ISBN 0-471-49369-4. Wiley-VCH, May 1974., 992 (1974).

- [26] R. Devi, P. Kalita, P. Purkayastha and B. Sarma, Indian Journal of Physics **82**, 707-713 (2008).
- [27] S. Horoz and O. Sahin, Journal of Materials Science: Materials in Electronics **28** (23), 17784-17790 (2017).
- [28] M. Maleki, M. Sasani Ghamsari, S. Mirdamadi and R. Ghasemzadeh, Semiconductor Physics, Quantum Electronics & Optoelectronics **10**, 30-32 (2007).